

# The Population of Mars-Crossers: Classification and Dynamical Evolution

Patrick Michel

*Osservatorio Astronomico di Torino, I-10025 Pino Torinese, Italy; and Observatoire de la Côte d'Azur, B.P. 4229, 06304 Nice cedex 4, France*  
E-mail: michel@obs-nice.fr

Fabbio Migliorini†

*Osservatorio Astronomico di Torino, I-10025 Pino Torinese, Italy; and Armagh Observatory, College Hill BT61 9DG, Northern Ireland, United Kingdom*

Alessandro Morbidelli

*Observatoire de la Côte d'Azur, B.P. 4229, 06304 Nice cedex 4, France*

and

Vincenzo Zappalà

*Osservatorio Astronomico di Torino, I-10025 Pino Torinese, Italy*

Received December 23, 1998; revised January 3, 2000

Recent dynamical results (Gladman *et al.* 1997. Dynamical lifetimes of objects injected into asteroid belt resonances. *Science* 277, 197–201) have pointed out that the bodies injected by collisions into the main resonances of the asteroid belt could not sustain the observed population of Earth-crossers of large diameter. In this paper, we present our numerical exploration of the dynamical evolution of Mars-crosser asteroids initiated by Migliorini *et al.* (1998. Origin of multikilometer Earth and Mars-crossing asteroids: A quantitative simulation. *Science* 281, 2022–2024.) and improved by computing the evolution over 100 Myr of the orbits of the whole observed sample of this population. Mars-crossers are about 35 times more numerous than Earth-crossers (at least down to 5 km in diameter). On the basis of their current orbital elements, we show that this population can be divided in different groups which have well-characterized dynamical behaviors, lifetimes, and end-states. From the dominant group, the asteroids evolve to intersect the Earth's orbit on a median time scale of about 60 Myr. Then, they can interchange between the Earth-crosser state and an evolved solely Mars-crosser one before colliding with the Sun or being ejected outside Saturn's orbit. Based on these dynamical results, we show that Mars-crosser asteroids can sustain about half of the multikilometer Earth-crossing population, and the expected orbital distribution of Earth-crossers coming from Mars-crossers is computed. Then, from an estimate of the size distribution of the Mars-crosser population and the spectral analysis of its different groups, we derive expected numbers of Earth-crossers and ratios of different taxonomic types in the Earth-crosser population that are not in disagreement

with the observed ones. We also confirm by spectral analysis the viability of the scenario, according to which the Mars-crosser population is sustained by asteroids which leak out from the main belt. © 2000 Academic Press

**Key Words:** asteroids, dynamics; planetesimals; resonances; surfaces, asteroids.

## 1. INTRODUCTION

The population of the  $\approx 400$  known near-Earth asteroids (NEAs) is composed of small bodies whose orbits currently cross or come close to that of the Earth. They are usually divided in three groups called Aten, Apollo, and Amor, depending on their current osculating orbital elements. Aten and Apollo asteroids evolve on orbits which currently cross the orbit of the Earth (with perihelion distance  $q < 1.017$  AU), whereas Amor asteroids are solely Mars-crossers though they can come close to the Earth (with  $1.017 < q < 1.3$  AU). However, the real population of Mars-crossers is not limited to the Amor group and their number is actually much larger than the number of NEAs. In this paper, we report in detail our study of the dynamical evolution of the Mars-crosser population. Preliminary results of this study, based on a restricted sample of this population, have already been presented by Migliorini *et al.* (1998). They are now improved thanks to the numerical integration of the whole known Mars-crosser population. As we will show, our results suggest that this population may not be able to sustain all multikilometer Earth-crossers in a steady state, but at least half of the current number.

† Died on November 2, 1997, in a mountain accident. This paper is devoted to his memory.

As a first step, we define as Mars-crossers all the bodies which are not presently Earth-crossers but intersect the orbit of Mars within the next precession cycle of their orbit. To identify most of the Mars-crossers, we have integrated for  $3 \times 10^5$  year the evolutions of all the known asteroids in the 1997 update of Bowell's catalog (Bowell *et al.* 1994) with present perihelion distance smaller than 1.78 AU. A body is considered a Mars-crosser if it passes through the torus defined by the heliocentric distance  $r$  between 1.341 and 1.706 AU, and vertical coordinate  $|z| < r \sin(6.4^\circ)$ . These bounds account for a martian maximal eccentricity of 0.12 and a maximal inclination over the invariable plane of  $6.4^\circ$ . Even excluding the objects currently located in main resonances, the Mars-crosser population contains 1460 members, about 354 of which are larger than 5 km in diameter. Undergoing close encounters with Mars, all these bodies are unstable and may potentially evolve to Earth-crossing orbits. To study their evolution and the possibility that they could be the dominant intermediate reservoir of Earth-crossers, we have numerically integrated all of them over a time scale of 100 Myr, using the `swift_rmvs3` numerical integrator designed by Levison and Duncan (1994).

According to the scenario developed by Wetherill (1985, 1987, 1988), which was reviewed with some personal interpretation by Greenberg and Nolan (1989), Earth-crossing asteroids are fragments of larger main belt bodies; as a result of the collisions which liberated them from their parent bodies, they were injected into one of the main resonances. These resonances, mainly the 3/1 mean motion resonance with Jupiter (which occurs when the orbital period of the asteroid is equal to 1/3 of the jovian period), and the  $\nu_6$  secular resonance (which occurs when the mean precession rate of the asteroid's perihelion equals that of Saturn) increased the orbital eccentricities of the resonant bodies until they started to cross the terrestrial planets' orbits. The encounters with the terrestrial planets could then extract them from resonances and spread them all over the Earth-crossing space, where they are now observed and categorized as NEAs. An alternative model by Greenberg and Chapman (1983, see also Greenberg and Nolan 1989) assumed that more numerous weak resonances also played a significant role.

Recent studies (Gladman *et al.* 1997) have shown that the median lifetime of bodies placed in the 3/1 or  $\nu_6$  resonances is only 2 Myr, i.e., one order of magnitude shorter than what was previously believed. Indeed, these resonances efficiently pump the eccentricity up to unity and lead most of the resonant bodies directly into the Sun. Therefore, to sustain via these resonances the population of Earth-crossing asteroids (denoted hereafter ECs)—also characterized by a short dynamical lifetime ( $<10$  Myr)—in a steady state, the number of bodies injected into the resonance per unit of time would need to be much larger than previously assumed. While this may still be plausible for small bodies (up to 1 km in size) the scenario becomes unrealistic for multikilometer asteroids (Menichella *et al.* 1996, Gladman *et al.* 1997) for the following reason. Ten bodies larger than 5 km are presently known to be on Earth-crossing orbits, i.e. with peri-

helion and aphelion distances, respectively, smaller and larger than 1 AU, and this number is multiplied by 2.5 if the bodies which will become ECs within one precession cycle of their orbits are also considered. These numbers are based on the 1997 update of the asteroids catalogue (Bowell *et al.* 1994), and the diameters have been estimated assuming the albedos reported in Migliorini *et al.* (1998, Table I), or IRAS measurements were available. Since the collisional injection of such bodies into resonances is rare, these considerations motivated our search for another source of multikilometer Earth-crossers.

Preliminary simulations by Migliorini *et al.* (1998) had suggested that the Mars-crosser population could sustain the Earth-crosser one with sizes larger than 5 km. To quantify, the number of bodies larger than 5 km expected to be found on Earth-crossing orbits was computed as a function of time, starting from a restricted sample of the present Mars-crosser population and assuming that this population is also maintained in a steady state. The authors found (see Migliorini *et al.* 1998, Fig. 3a) that the produced number of ECs oscillates with an average value in very good agreement with that presently observed (10 bodies). Thus the conclusion was that, from the quantitative viewpoint, the Mars-crossing population can be considered as the main intermediate source reservoir of multikilometer ECs. We have then updated these results by enlarging the sample of Mars-crossers studied by Migliorini *et al.* (1998) to their total number. The results exposed in the present paper suggest that the Mars-crosser population is actually able to sustain half of the current number of Earth-crossers larger than 5 km in size.

Given the undoubtedly important contribution of Mars-crossers in the population of ECs, we have extended this study in order to obtain a description of their dynamical evolution and our results are also reported in the present paper. We have first divided Mars-crossers in different dynamical groups and have then examined their dynamical evolutions. This approach has allowed us to get a good description of the main dynamical behaviors for each defined group, and thus to better understand how Mars-crossers are transported to Earth-crossing orbits, as well as the interplay between these two populations (see the conclusion and Fig. 14 for a schematic view of the global scenario).

In Section 2, we present our definitions of the different groups of Mars-crossers based on dynamical considerations. Section 3 is devoted to a detailed study of the dynamical evolutions of each group separately, allowing us to distinguish different dynamical behaviors. In Section 4, we present the updated result on the number of Earth-crossers sustained by the Mars-crosser population. Section 5 is devoted to an analysis of the taxonomic distribution of each Mars-crosser group in order to compute the expected ratio of the different taxonomic types in the EC population. This ratio is then compared with the observed one. Section 6 discusses the scenario for the origin of Mars-crossers and compares the taxonomic distributions in the Mars-crossing populations with those in the non-Mars-crossing asteroidal populations. The conclusions are then presented in Section 7.

## 2. CLASSIFICATION OF MARS-CROSSERS ACCORDING TO THEIR ORBITAL DISTRIBUTION

In this section, we present our classification of the Mars-crossers based on their current orbital distribution. As we shall see later (Section 3), this classification is useful for distinguishing different dynamical behaviors, lifetimes, and end-states.

Figure 1 shows the orbital distribution of the Mars-crossers with respect to current semimajor axis and inclination. In the following, we give a qualitative description of the different groups and then their exact limits in semimajor axis and inclination.

One can see (Fig. 1) that three main groups are easily identified, with values of semimajor axis  $a$  and inclination  $i$  similar to those of three populations of non-planet-crossing asteroids, the main belt below the  $\nu_6$  resonance, the Hungarias and the Phocaeas. We denote them MB, HU, and PH Mars-crossers. This similarity suggests that the non-planet-crossing populations might be continuously losing objects to the Mars-crossing region, sustaining the MB, HU, and PH groups. This has already been confirmed recently by Migliorini *et al.* (1998), whose results will be briefly recalled in Section 6. Among the remaining Mars-crossers, those on the left of the 4/1 resonance with Jupiter have orbital elements which differ from those of all non-planet-crossing asteroidal populations. Therefore they have probably evolved relative to the orbit that they had when they first crossed the orbit of Mars (this will be confirmed later in Section 3.6): for this reason we denote them EV. Finally, the Mars-crossers on the right of the 3/1 and above the  $\nu_6$  resonances could be related to the non-planet-crossing asteroids located in this region: we refer to them as MB2.

We define the exact limits in semimajor axis and inclination of each group as follows:

- MB are Mars-crosser asteroids with  $a > 2.06$  AU (location of the 4/1 resonance with Jupiter) and an inclination such that they are below the  $\nu_6$  secular resonance;
- HU have  $1.77 < a < 2.06$  AU and  $i > 15^\circ$ ;
- PH have  $2.1 < a < 2.5$  AU (between the 4/1 and 3/1 resonances with Jupiter) and are situated above the  $\nu_6$  secular resonance;
- MB2 have  $a > 2.5$  AU and are situated above the  $\nu_6$  secular resonance;
- EV are Mars-crosser objects having either current semimajor axis  $a < 1.77$  AU (location of the 5/1 resonance with Jupiter) or  $1.77 < a < 2.06$  AU (i.e. between the 5/1 and 4/1 resonances with Jupiter) and inclination  $i < 15^\circ$ .

The limits in semimajor axis of the whole Mars-crosser population are at about 1.3 and 2.8 AU. Below 1.3 AU asteroids cannot intersect the orbit of Mars without being ECs. Beyond 2.8 AU, being a Mars-crosser implies an aphelion distance larger than 4 AU, which makes a removal by Jupiter encounters very easy.

The numbers of MB, HU, PH, MB2, and EV Mars-crossers are listed in Table I. An important point is that by integrating

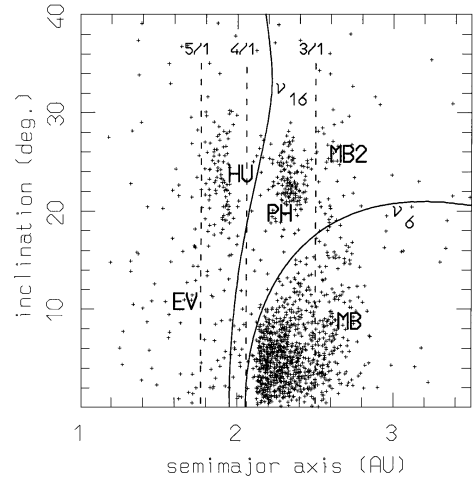


**FIG. 1.** Orbital distribution of Mars-crossers (inclination vs semimajor axis). Labels denote the different groups described in the text. The two curves denote the location of the  $\nu_6$  and  $\nu_{16}$  secular resonances; the dashed lines correspond to the positions of the 5/1, 4/1, and 3/1 mean motion resonances with Jupiter.

**TABLE I**  
**Summary of the Numerical Integrations over 100 Myr**

	MB	HU	PH	MB2
Total no. of bodies:	1039	114	165	37
No. with $D > 5$ km (%):	240 (23.1)	17 (25.0)	78 (100.0)	12 (75.0)
No. of effective MCs:	885	68	78	16
Outside Saturn (%)	155 (26.2)	2 (10.5)	0	3 (27.3)
Impact Sun (%)	395 (66.8)	15 (78.9)	21 (95.4)	7 (63.6)
Half-life (Myr)	62.4	>100. (27.9)	>100. (28.2)	44.4
No. of EC (%)	591 (66.8)	33 (48.5)	24 (30.8)	12 (75.0)
$T_{cr}$ Earth (Myr)	59.9	>100.	>100.	37.6
Ever have $a < 2$ AU (%)	191 (21.6)	67(98.5)	10 (12.8)	0
$T_{mean}$ (Myr)	7.9	67.3	2.8	—
Ever have $a < 1$ AU (%)	24 (2.71)	1 (1.47)	0	0
$T_{mean}$ (Myr)	10.4	6.9	—	—
Ever have $Q < 2$ AU (%)	54 (6.1)	37 (54.4)	0	0
$T_{mean}$ (Myr)	10.3	18.37	—	—
Ever have $Q < 1$ AU (%)	17 (1.92)	1 (1.47)	0	0
$T_{mean}$ (Myr)	5.46	0.11	—	—

*Note.* Each class of objects is defined by its label. Effective MCs are objects which suffer at least one encounter inside Mars's Hill sphere within the 100-Myr time span. Statistics are computed only from the latter, noneffective Mars-crossers remaining in their initial state during the whole time span. The table shows the number of bodies which are ejected beyond Saturn or which impact the Sun (the percentage that they represent over the number of nonsurviving bodies is shown in brackets). Time scales are shown for 50% (half-life) and median times  $T_{cr}$  for crossing the orbit of Earth. If more than 50% of small bodies survive over the integration time, the percentage of nonsurviving bodies in the effective MC population is given in parenthesis on the half-life line. At the bottom of the table, the number (percentage) of objects which are temporarily in regions of particular interest and the mean time spent in these regions ( $T_{mean}$ ) are listed. The value of  $Q$  indicates aphelion distance. Diameters are estimated assuming different albedos, 0.3 for HU (i.e., taking into account that most are bright E-type asteroids) and from 0.16 to 0.08 (depending on the semimajor axis) for the other classes.

the whole population of Mars-crossers identified as explained in Section 1, we found that several of them actually never have an encounter with Mars at a distance smaller than the corresponding Hill’s sphere radius of this planet during the 100 Myr time span. Consequently, we decide to define as *effective* Mars-crossers the particles which undergo at least one encounter within this distance over the 100 Myr time span, and to compute the statistics on the basis of this effective population. Noneffective Mars-crossers remain stable during the whole integration time. We have numerically integrated all Mars-crossers over a time span covering 100 Myr. We have then separated them in their corresponding groups and studied their evolutions.

### 3. DYNAMICAL EVOLUTIONS OF MARS-CROSSERS

In this section, we present the main characteristics of the evolutions, considering each group separately. We also show density plots of the NEA population that each of these groups should sustain, in a steady-state scenario.

#### 3.1. MB Group

The MB group is the most numerous group of MCs. In particular, our numerical simulations show that 50% of the MB Mars-crossers become ECs within 59.9 Myr and that the contribution of this group dominates the production of ECs (Migliorini *et al.* 1998).

We have also found that the time needed for an MB to become an Earth-crosser has on average a mild dependence on the initial perihelion distance  $q$ . Indeed, Fig. 2 shows, in the upper plot, the time to reach the Earth-crossing region (in log-scale) as a function of the initial perihelion distance of MB members. The asteroids that do not become Earth-crossers within the integration time have been disregarded. MBs indicated by a blank circle have a short Earth-crossing time ( $<10^7$  year), whereas their initial perihelion distance  $q$  is greater than 1.65 AU. This is mainly due to the fact that their initial semimajor axis is already very close to a resonant value, so that they are quickly transported to the Earth-crossing region. Moreover, all these objects have a small inclination ( $i < 10^\circ$ ) and can only encounter Mars when the planet is close to its aphelion (presently located at 1.67 AU). In this case, the two orbits are almost tangent during an encounter, and, consequently, the effects of the encounters may be particularly large and drive the asteroid more efficiently into a resonance. Eliminating these asteroids, which initially can be easily identified, one can see that the time to become EC tends to linearly increase (in log-scale) as  $q$  becomes larger, until  $q = 1.6$  AU, and then it is an almost constant function of  $q$ . In order to better show this trend, we have applied a running box method to the data represented by the bold dots: we considered 20 boxes of equal sizes in perihelion distance and computed the average and standard deviation of the time needed to become EC in each box. The result of this exercise is shown in the lower panel of Fig. 2. Though the transport efficiency actually depends on many parameters such as semimajor axis and inclination val-

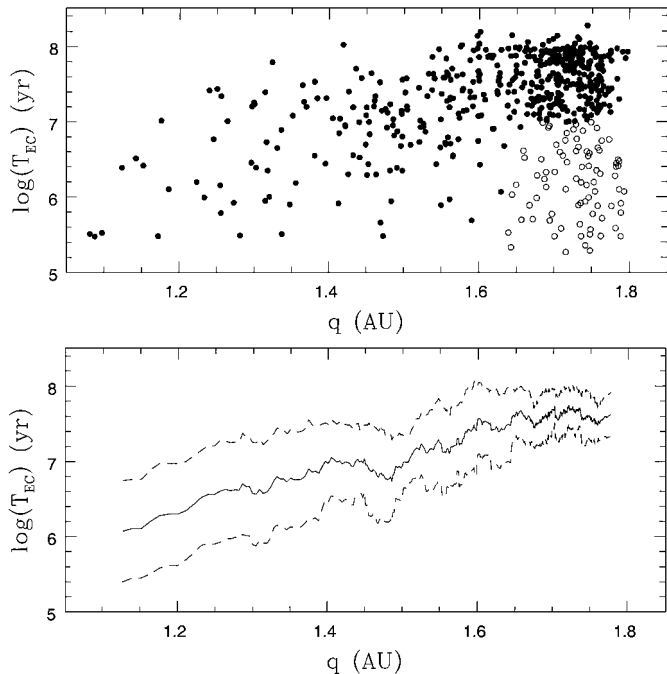


**FIG. 2.** The upper panel shows the time  $T_{EC}$  to become an Earth-crosser (in log-scale) vs initial perihelion distance  $q$  (in AU) for MB Mars-crossers. The asteroids that do not become Earth-crossers within the integration time are not represented. We have applied a running box method to the data represented by the filled circles to compute the mean and the standard deviation. The latter are represented by the solid and the dashed lines in the lower panel.

ues, which indicate the proximity to a powerful resonance and the frequency of encounters with Mars, this plot shows that the knowledge of the initial perihelion distance can already give an approximate indication of the average time required to reach the Earth-crossing zone.

However, several MBs ( $\approx 37\%$  of the *effective* MB group) never become ECs within the 100-Myr integration time span. We expect these objects to eventually be transported to the Earth on a longer timescale. Their existence shows that the Mars-crossing population can have some old components which stay “parked” in the Mars-crossing region for several hundred Myr.

Concerning MBs which become ECs, we find that this typically happens by random-walking in semimajor axis under the effects of close encounters with Mars until entering into some secular or mean motion resonance which increases the eccentricity to an Earth-crossing value. In our sample, about 40% of the asteroids are transported by the 3/1 resonance, 40% by the  $\nu_6$  resonance and/or the 4/1 resonance with Jupiter, and 20% by other routes (mostly higher-order resonances). The dynamical half-life of the MBs is about 62 Myr, the typical end-states being collision with the Sun or ejection on hyperbolic orbit by Jupiter encounters. Moreover a large fraction of them ( $\approx 21.6\%$ ) temporarily reach a semimajor axis smaller than 2 AU, typical of many ECs, and a nonnegligible component ( $\approx 3\%$ ) even achieves Aten-like orbits with  $a < 1$  AU. Note that using these integrations, Michel *et al.* (2000) have already shown that the

MB population could be at the origin of a nonnegligible fraction of Inner-Earth Objects (IEOs, defined as asteroids with  $a < 1$  AU and aphelion distance  $Q < 0.983$  AU) in the Earth-crossing population. Indeed, assuming that, in a steady-state scenario, the number of objects in different regions of the Earth-crossing space is proportional to the times spent in these regions by particles coming from the MB population considered here as the only source (such a method will also be discussed in Section 3.5 of the present paper), they found that the ratio IEO/Aten objects coming from the MB group could be as much as 0.6, whereas no real IEO has been discovered yet.

Figures 3, 4, and 5 illustrate three evolutions of MB Mars-crossers that become ECs.

Figure 3 shows one of the few asteroids whose transport in the Earth-crossing region is not due to one of the main resonances (3/1, 4/1,  $\nu_6$ ) but rather due to close encounters with Mars and second-order secular mechanisms. The asteroid first evolves in the vicinity of the  $\nu_6$  and 4/1 resonances at  $a \sim 2.1$ –2.15 AU, which causes secular oscillations of the eccentricity within the time span  $10 < t < 14$  Myr. However, the eccentricity increase is not sufficient to decrease the perihelion distance below the Earth-crossing value. The asteroid then suffers a very close approach to Mars, jumping to  $a \sim 1.7$  AU and  $e \sim 0.2$ . At this point the body can be classified as an EV Mars-crosser. Subse-

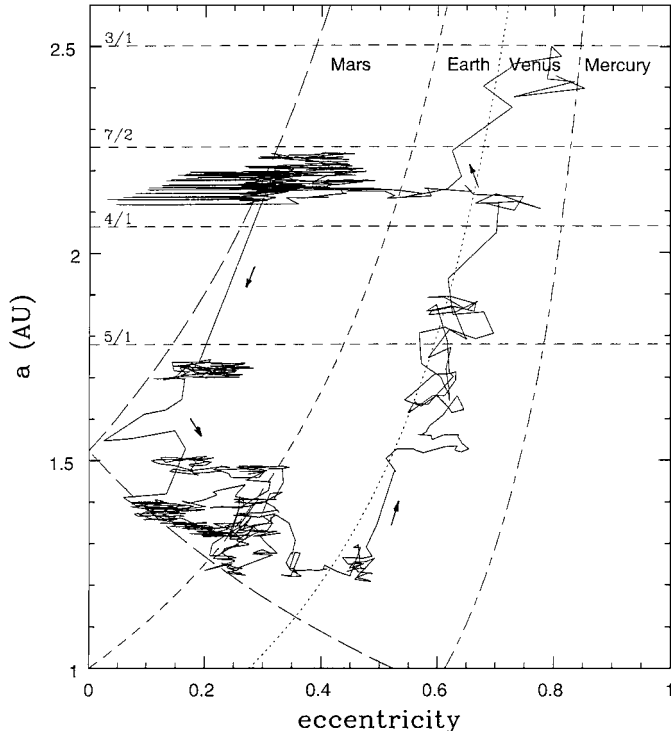


**FIG. 3.** The evolution in the semimajor axis ( $a$ , in AU) vs eccentricity ( $e$ ) plane of an MB Mars-crosser which becomes an Earth-crosser as a result of close approaches to Mars and second-order secular mechanisms. The direction of the evolution is sketched by the arrows. The horizontal lines correspond to main mean motion resonances with Jupiter.

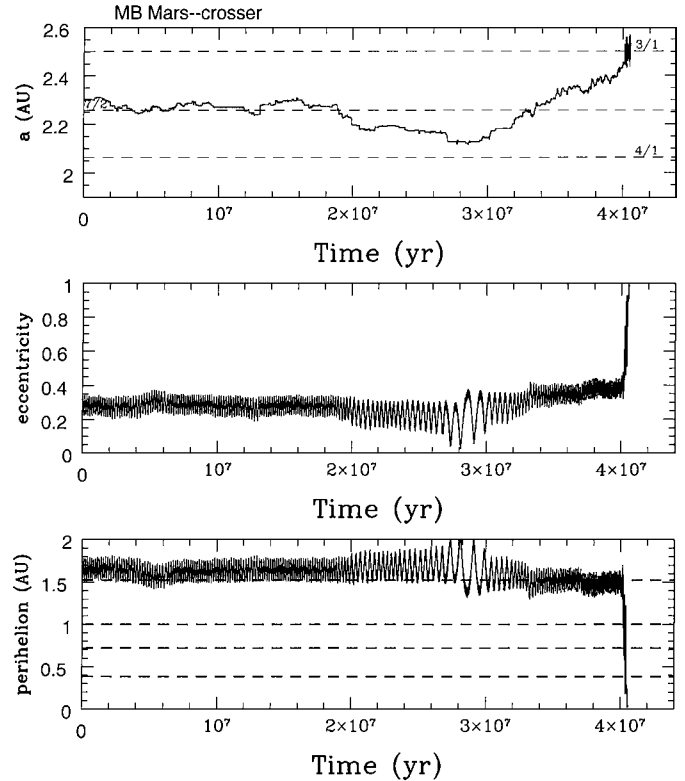


**FIG. 4.** Time evolutions of the semimajor axis  $a$  (AU), eccentricity  $e$ , and perihelion distance  $q$  (AU) of an MB Mars-crosser which becomes an Earth-crosser after its injection into the 3/1 resonance. In the semimajor axis plot, the dashed lines show the location of the main mean motion resonances with Jupiter.

quent encounters with Mars then rapidly transport the body to  $a \sim 1.5$  AU, where secular resonances of second order increase its eccentricity above the Earth-crossing limit at  $t \approx 22$  Myr. Encounters with the Earth then transport the body to  $a \sim 1.3$  AU, where its eccentricity is temporarily decreased again below the Earth-crossing value, probably by martian encounters. In this phase, the asteroid would belong again to the EV Mars-crossing group. Finally, the asteroid becomes a deep Earth-crosser (at  $t \approx 34$  Myr) due to a secular increase of the eccentricity related to second-order secular mechanisms, and encounters with the Earth and Venus transport it back toward the main belt ( $a \sim 2$  AU). It is finally thrown into the Sun by the  $\nu_6$  resonance after about 40 Myr of evolution. The kind of dynamical evolution shown in Fig. 3 is not common. Nevertheless, its existence shows that main resonances are not the only path to the Earth.

Conversely, Fig. 4 shows an asteroid which becomes EC due to its transport by martian encounters in the 3/1 mean motion resonance with Jupiter. During the first 20 Myr, its semimajor axis evolves very close to the value corresponding to the 7/2 resonance with Jupiter ( $a \approx 2.27$  AU), but the asteroid is never trapped in the resonance. Since the perihelion distance oscillates in and out of the Mars-crossing region, the asteroid undergoes close encounters with Mars which slowly affect its semimajor axis until it goes into the 3/1 resonance with Jupiter. Once in the

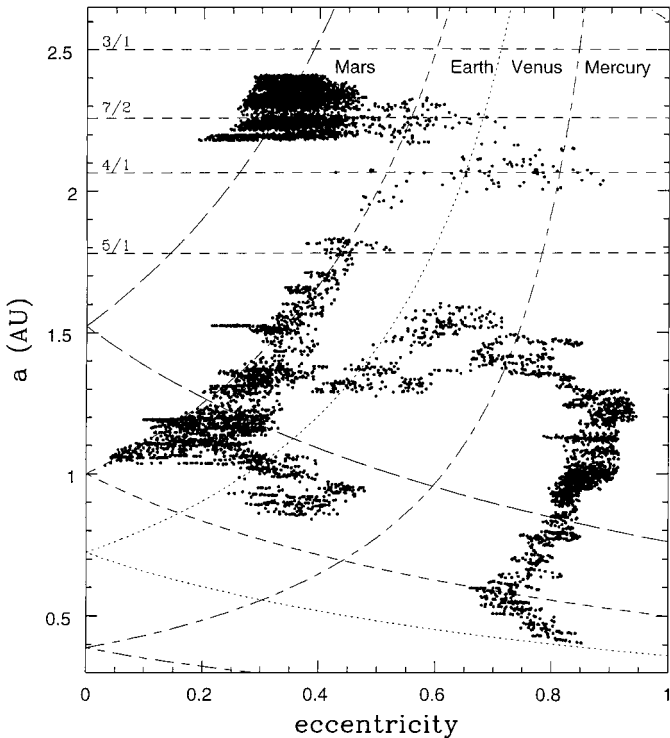


**FIG. 5.** Same as Fig. 3 for an MB Mars-crosser which becomes an Earth-crosser and then evolves to the Aten region ( $a < 1$  AU), where it then collides with Venus.

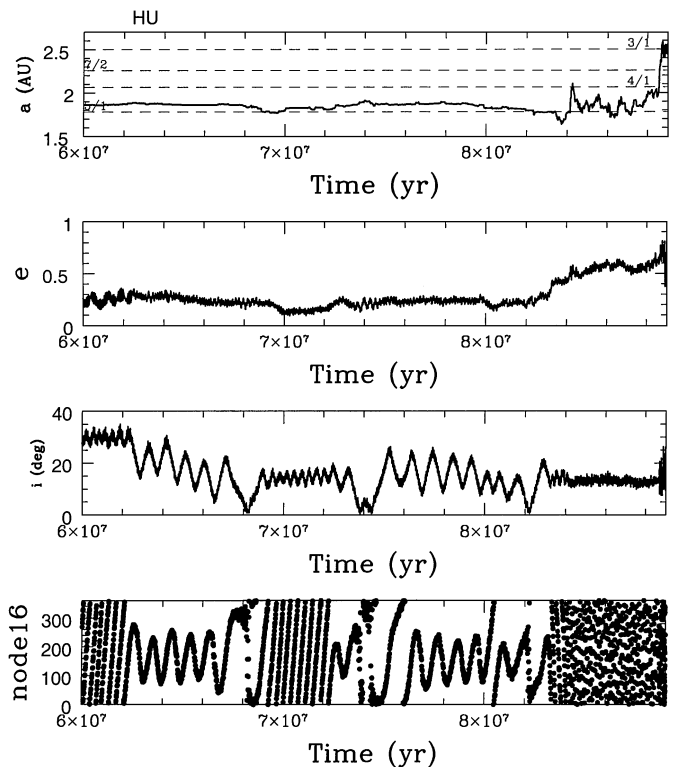
resonance, it suffers a drastic increase of the orbital eccentricity and collides into the Sun after 40.5 Myr of evolution. This object becomes an Earth-crosser only for a short time on its way to the Sun, as already typically found by Gladman *et al.* (1997) for fragments injected into the 3/1 resonance.

Figure 5 shows the evolution of an asteroid which becomes and then remains EC for almost 50 Myr. During the first  $\approx 45$  Myr, it evolves on a solely Mars-crossing orbit. Then a close approach to Mars injects it into the 7/2 resonance with Jupiter which increases its eccentricity up to an Earth-crossing value. Encounters with the Earth are efficient enough in this case to extract the asteroid from the resonance. It then evolves in the Earth-crossing region, undergoing close approaches with the Earth. A passage through the 4/1 resonance decreases the eccentricity of the body, to bring its perihelion close to 1 AU. Then, the body is transported along a  $q \sim 1$  AU curve, and the eccentricity oscillations make the asteroid continuously exchange from the EC to the EV states and vice versa. When  $a \sim 1$  AU the eccentricity increases as a consequence of close approaches and secular resonances located in this region (Michel and Froeschlé 1997) and brings the body to the Venus-crossing region. The body then jumps back to  $a \sim 1.5$  AU, where the eccentricity further increases. Subsequent planetary encounters then slowly drift its semimajor axis below 1 AU, so that it finally evolves on an Aten-like orbit ( $a < 1$  AU). It remains in this state during several tens of millions of years until it collides with Venus. We emphasize that we have found this

kind of evolution quite frequently in our simulations. Actually, about 3% of MBs reach an Aten-like orbit.

### 3.2. HU Group

Mars-crossers belonging to the HU group become ECs on longer time scales, due to the reduced strength and frequency of encounters with Mars at high orbital inclinations. Within the integration time span (100 Myr), 51.5% of the effective HUs never become ECs. Nevertheless, about 1.5% of the integrated HU asteroids reach the Aten region. Figure 6 shows an evolution which is typical of HU asteroids that become Earth-crossers. Very few HUs become EC without first being EV, i.e., Mars-crossers with  $a < 2$  AU and  $i < 15^\circ$ . Indeed, due to the proximity of the  $\nu_{16}$  resonance (which occurs when the mean precession rate of the asteroid's node equals that of Jupiter's), HU Mars-crossers first become EVs due to a decrease of their inclination. Such behavior is shown in Fig. 6 by the libration of the  $\nu_{16}$  resonant critical argument around  $180^\circ$ . Actually, the injection in the resonance is related to the position of the semimajor axis. As one can see on the figure, the first libration of the resonant angle occurs at time  $t = 62$  Myr after a slight increase of the semimajor axis. Then, when this element decreases again, the asteroid leaves the



**FIG. 6.** Time evolution of an HU Mars-crosser which becomes an Earth-crosser. Beside semimajor axis  $a$ , eccentricity  $e$ , and inclination  $i$ , the bottom panel also shows the critical argument ( $\Omega - s_6 t - \beta_6$ ) of the  $\nu_{16}$  secular resonance ( $\Omega$  is the nodal longitude of the asteroid,  $s_6 = -26.3302$  arcsec/year is the fundamental frequency corresponding to the resonance, and  $\beta_6$  is the phase at  $t = 0$ ). Note the repeated passages through the resonance that affect the inclination.

resonance (at  $t \approx 69$  Myr) and the angle circulates. A slight increase of the semimajor axis reinjects it into the resonance (at  $t \approx 73$  Myr).

Once the inclination is smaller, close approaches to Mars can be more frequent and efficient. Consequently, the changes in semimajor axis can inject the body into a resonance which increases the orbital eccentricity up to an Earth-crossing value. In our example (Fig. 6), this happens through the 5/1 resonance with Jupiter at about  $t \sim 82$  Myr. Then close approaches to the Earth, combined with some secular mechanisms (here the  $\nu_3$  and  $\nu_4$  secular resonances with the Earth and Mars) affect, respectively, the semimajor axis and the eccentricity until the asteroid finally enters deeply in the 3/1 resonance with Jupiter. It is eventually driven into the Sun after 94 Myr of evolution.

We finally want to point out (see also Section 3.6) that several evolutions of the other Mars-crosser groups suggest that some objects currently characterized as HU Mars-crossers may actually be EV *interlopers*, i.e., previous EVs which are evolving temporarily in the HU region as a result of an increase of their inclinations. Therefore, the real number of *primordial* HU Mars-crossers (defined as bodies which became Mars-crossers for the first time as HU members) may be smaller than the one derived from the current orbital elements of Mars-crossing asteroids. However, our simulations suggest that EV Mars-crossers entering in the HU region evolve in this state only during a short time span. Therefore, it is reasonable to think that HU members which have a long lifetime and which do not become Earth-crossers within the 100 Myr integration time (the majority of the integrated HU group) are not interlopers.

### 3.3. PH Group

Among the different groups constituting the Mars-crosser population, the PH group is the most stable one. Indeed, though PH asteroids have a semimajor axis located between the 4/1 and 3/1 resonances, they also have a high inclination (i.e., above the  $\nu_6$  resonance). Therefore, close approaches with Mars happen at low frequency and high relative velocities, decreasing thus the probability of great changes in semimajor axis. Consequently, the lifetime of this group is longer than the integration time span and only 31% of the objects reach the Earth-crossing zone in 100 Myr. As for MB asteroids, the usual transport mechanism to the Earth-crossing region is one of the main resonances with Jupiter located in proximity (e.g., 4/1, 3/1, or 7/2).

### 3.4. MB2 Group

The typical evolutions of MB2 asteroids are qualitatively similar to those of MB asteroids, but given their initial semimajor axis ( $a > 2.5$  AU), the resonances transporting them are preferentially the 3/1, 8/3, 7/3, and 5/2 with Jupiter. Evolving closer to the Jupiter-crossing region, their ejection outside Saturn's orbit as a result of a jovian encounter is more probable than for the other groups. For this reason the MB2s do not contribute much to sustain the Earth-crossing population. None of the MB2s that

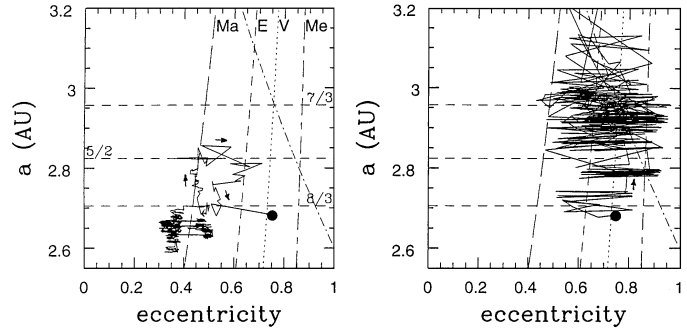


**FIG. 7.** Same as Fig. 3 for an MB2 Mars-crosser that is eventually ejected outside Saturn's orbit. The left panel shows the evolution until time  $t = 24.33$  Myr (represented by a bold dot). The right panel shows the evolution starting from this time (indicated by the bold dot).

we have integrated ever reaches semimajor axes smaller than 2 AU. The half-life of MB2s (45 Myr) is shorter than that of the MB group though the high inclination of their orbits (located above the  $\nu_6$  resonance) decreases the efficiency and frequency of martian encounters. Nevertheless, MB2s are less stable than the MBs and the PH group also situated above the  $\nu_6$  resonance. Indeed, to be Mars-crosser with a semimajor axis  $> 2.5$  AU implies having a large eccentricity and being close to Jupiter's orbit.

Figure 7 shows an example of evolution. The body has initially  $a \sim 2.6$ – $2.7$  AU and is barely Mars-crossing. The two parallel bands at about  $e = 0.35$  and  $e = 0.5$  are an artifact of our output method, which tends to cluster the data around the minimal and the maximal eccentricity reached during the precession of the argument of perihelion. The encounters with Mars transport the asteroid into the 5/2 resonance, in which the eccentricity increases to Earth-crossing values. Then its eccentricity decreases again so that the body comes back to the MB2 state. It is being transported back toward its original position, when the 8/3 resonance increases its eccentricity again up to the Earth-crossing value (Fig. 7, left panel). Then, planetary close approaches rapidly increase its semimajor axis toward 3 AU (Fig. 7, right panel). Consequently, its aphelion being closer to Jupiter's orbit, a close approach with this planet occurs and ejects the asteroid outside Saturn's orbit. Less than 2 Myr separate the first Earth-crossing episode from the final ejection toward the outer Solar System.

### 3.5. Steady-State Orbital Distribution of NEAs Coming from the Mars-Crossing Groups

In this section, our aim is to present a global view of the evolutions of Mars-crossers of each group in the Earth-crossing zone, defined as a target region. For this purpose, we divide the  $(a, e, i)$ -space into cells of equal size (0.1 AU in  $a$ , 0.05 in  $e$ , and  $5^\circ$  in  $i$ ) and compute the total time spent by the integrated bodies in each cell. In this way, we obtain a density distribution in the  $(a, e, i)$ -space, whose projections on the  $(e, a)$  and  $(i, a)$  planes are shown in Figs. 8 to 11 separately for particles initially in the MB, HU, PH, and MB2 groups. The residence

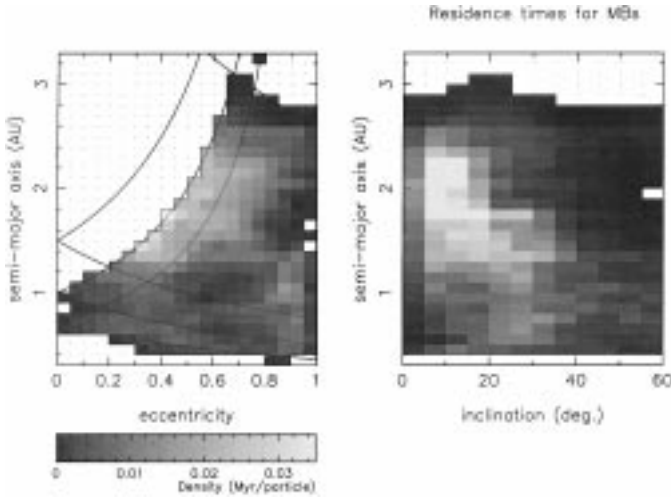


**FIG. 8.** Mean residence time in the Earth-crossing region of bodies initially in the MB group. The gray-scale gives the average time spent (Myr per particle extracted from the source region) in the different cells, the darkest being the shortest. Blank spaces correspond to regions where no time has been spent.

time has been normalized by the number of integrated particles which are extracted from their source region defined by the corresponding limits in orbital elements of their initial group. Thus these residence times represent the total amount of time a particle spends in the various regions of the orbital element space during its evolution once extracted from its source region. In a steady-state scenario, these plots represent the expected orbital distribution of the bodies that come from the different Mars-crossing groups (Bottke *et al.* 1996). Indeed, the probability of finding an object in a given cell is evidently proportional to the total time spent in that cell by the integrated test particles. Note that, strictly speaking, this is true only outside of the source region, since many particles may have already spent some time in their region of origin before being observed, justifying our

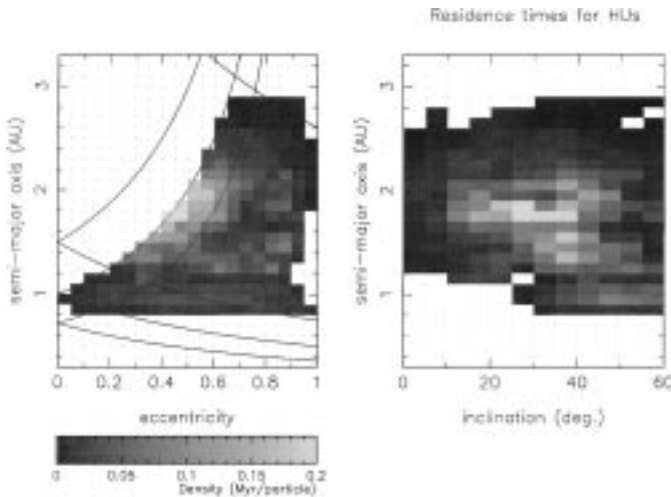


**FIG. 9.** Same as Fig. 8 for bodies initially in the HU group.

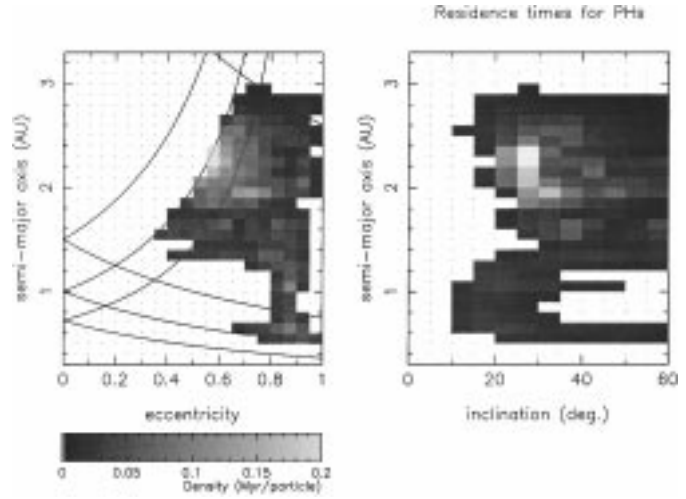


**FIG. 10.** Same as Fig. 8 for bodies initially in the PH group.

choice not to consider the source in the computation of the residence times.

The density distribution of bodies originally in the MB group (Fig. 8) shows a concentration at perihelion distances close to 1 AU. Although most of the MBs become ECs through the 3/1 or the  $\nu_6$  resonances, the density plots of main belt particles initially placed in these resonances (Morbidelli and Gladman 1998) do not show such a prominent concentration at  $q \sim 1$  AU. Actually, the difference comes from the fact that when the MBs approach the  $\nu_6$  resonance, the secular oscillation amplitude of their eccentricity slowly increases, so that they become ECs with  $q \sim 1$  AU before having a chance to enter deeply into the resonance. Close encounters with the Earth are then very efficient and transport the bodies along the  $q \sim 1$  AU curve, as in Fig. 5. Conversely, the bodies initially placed in the 3/1 or  $\nu_6$  resonance have their eccentricity increased so rapidly to large values that the first encounters with the Earth happen already when their

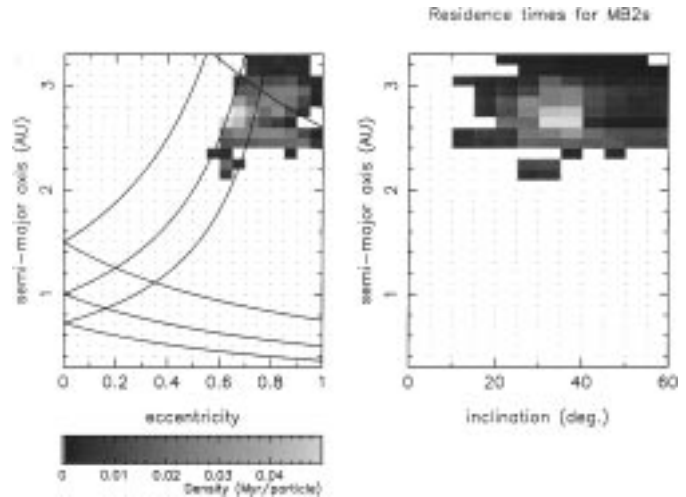


**FIG. 11.** Same as Fig. 8 for bodies initially in the MB2 group.

perihelion distance is much smaller than 1 AU. Figure 8 also shows that the bodies coming from the MB group, when in the region with  $a < 2$  AU, have a typical inclination ranging from  $5^\circ$  to  $30^\circ$ . We remark also a non-zero residence time in the Aten region ( $a < 1$  AU), with a small concentration at high eccentricities ( $> 0.8$ ). Finally, we note that the mean time spent in the Earth-crossing zone with  $a < 2$  AU by the MB group ( $\approx 8$  Myr) is similar to the 9 Myr median lifetime of the sample of observed Earth-crossers numerically integrated by Gladman *et al.* (2000), which included 66% of particles initially with  $a < 2$  AU.

Figure 9 shows the residence times of HU Mars-crossers. We remark a concentration at the border of the Earth-crossing region with  $a = 1.5\text{--}2$  AU and  $i = 5\text{--}15^\circ$ , due to the fact that, as described in Section 3.2, most of the HU Mars-crossers first escape from their source region by decreasing the inclination under the effect of the  $\nu_{16}$  secular resonance. Only a small fraction of the total time is actually spent on an Earth-crossing orbit by the bodies originally in the HU group, as was reasonable to expect since the median time to become an Earth-crosser is greater than 100 Myr while the typical lifetime after the first Earth-crossing episode is much shorter.

Figures 10 and 11 show the same plots for PH and MB2 Mars-crossers. These plots are both characterized by a residence time at the border of the Earth-crossing zone close to their source region that is much larger than that in the other parts of the Earth-crossing region. This is due to their large inclination ( $i > 20^\circ$ ) which makes encounters with Mars inefficient to rapidly inject them into a transporting resonance. Also, the vicinity of the Kozai resonance at high inclinations causes wide oscillations of the eccentricity which allow the particles to undergo shallow and temporary excursions into the Earth-crossing zone when the eccentricity is near the peak of its cycle. Such behavior has already been studied in the particular case of (1036) Ganymed (Michel *et al.* 1999), which belongs to the MB2 group. Moreover, for this group, the lifetime in the Earth-crossing region is particularly short, because of the vicinity of Jupiter. We remark that both PHs and MB2s decrease their semimajor axis to small values with great difficulty. No MB2s are found to be transported to  $a < 2$  AU. Conversely, one PH has been found to reach the Aten region, but on a time scale longer than the 100 Myr integration time span performed for the whole population. This is the reason it is not indicated in Table I.

### 3.6. EV Group

We finally come to the discussion of the origin and fate of the EV Mars-crossers. Orbital elements of EV asteroids differ from those of all non-planet-crossing asteroidal populations. Therefore they must have evolved relative to the orbit that they had when they first crossed the orbit of Mars.

As already shown, several bodies belonging originally to MB or HU groups temporarily become EVs (see Figs. 3, 5, and 6). From our simulations, we conclude that EV Mars-crossing asteroids are mainly generated in two different ways. The first way applies to the MB Mars-crossers. Asteroids from this group first

become ECs, decrease their semimajor axis under the action of Earth (and Venus) encounters, and then temporarily decrease their eccentricity under the effect of some resonance. Secular resonances with the inner planets can be important in this phase (Michel and Froeschlé 1997, Michel 1997). Consequently, the perihelion distance is raised above the Earth-crossing limit, so that the previously Earth-crossing object goes back to the purely Mars-crosser state. Very few MBs become EVs without first being ECs.

The second way applies to the HU group: being located close to the  $\nu_{16}$  resonance, HU asteroids preferentially first decrease their inclination below  $15^\circ$ , becoming EVs (see Fig. 6) before eventually reaching an Earth-crossing orbit. However, we have also found that several MBs which become EVs once in this state have their inclinations increased so that they evolve temporarily in the HU group and then come back again to the EV state. As already pointed out in a previous section (Section 3.2), since the HU population has a very long lifetime, this suggests that some of the HU members with a short lifetime may actually be previous EV members placed temporarily in the HU region so that they are currently characterized as HU members. Consequently, our definition of the HU group based on current observations may lead to an overestimate of its members, affected by several EV interlopers. Primordial HU members, in the sense that they have never spent time in any other Mars-crossing state, may then actually be less numerous than in the observed sample.

In general terms, we can conclude that the EC and EV populations continuously interchange part of their members, because the eccentricity oscillations bring several asteroids alternatively in the EC and in the EV region, as shown for instance in Fig. 5. Consequently, it is reasonable to expect that large bodies presently in the EV region, such as (433) Eros, may have already spent some time in the Earth-crossing region. This is also discussed in Michel *et al.* (1998).

The bodies presently in the EV group have a 93-Myr half-life, longer than that of the MB group. This can be easily explained: having a semimajor axis located in the main belt, most MB asteroids are initially placed close to a dangerous resonance. Conversely, EVs, having a semimajor axis smaller than 2 AU, are far from any dangerous main belt resonance and survive a long time interval before they are transported to  $a > 2$  AU. Then, they either impact into the Sun or are ejected toward the outer Solar System. We also remark that 24.5% of the integrated EVs temporarily penetrate into the Aten region. This is in agreement with recent integrations over their lifetime of a sample of observed Apollo objects showing that 27% of them go into the Aten region (Michel *et al.* 2000), thus confirming the potential link between EVs and ECs.

## 4. NUMBER OF EARTH-CROSSERS SUSTAINED BY MARS-CROSSERS

Based on the numerical integrations of the orbits of a restricted sample of Mars-crossers, Migliorini *et al.* (1998) computed the

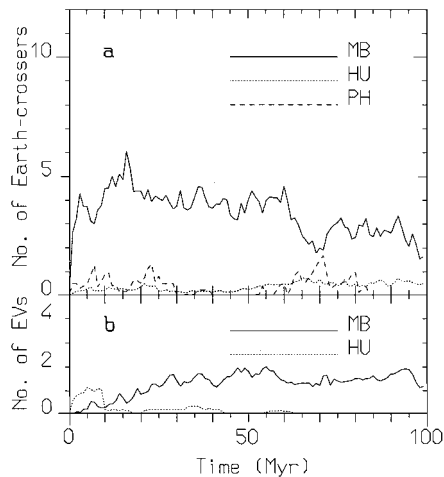


**FIG. 12.** Number of bodies with a diameter larger than 5 km expected on EC (a) and EV (b) orbits starting from the present MBs (solid line), HUs (dotted line), and PHs (dashed line). The contribution of MB2s is negligible.

number of Earth-crossers that each group of Mars-crossers could sustain in a steady-state scenario. They found that they were able to sustain the whole population of ECs with diameter greater than 5 km (10 asteroids). Since we have now integrated the total population of Mars-crossers, we have redone the computation using the same method. We have thus computed the number of bodies on EC and EV orbits sustained by the different groups as a function of time.

In order to directly compare these results with the previous ones by Migliorini *et al.* (1998), we have scaled the number of bodies down to reflect the results we would expect if we had started with the actual number of MCs with diameters larger than 5 km. Figure 12 shows the results of this exercise. As found by Migliorini *et al.* (1998), the number of ECs coming from the MC groups increases rapidly with time, because a fraction of MBs (those with initial  $q$  already close to 1 AU or who are rapidly captured by the 3/1 or  $\nu_6$  resonance) become EC on a short time scale. Then, between 10 and 60 Myr, the number of bodies oscillates mainly between 3 to 5 bodies. Finally, the number slowly decays due to the 60-Myr median lifetime of the MB group. Note that the contribution of the HU and PH populations is limited to about one Earth-crosser. This could be either real or due to the fact that the median time for these populations to become EC is longer than the considered 100-Myr time span.

As for EV bodies, about 2 objects are sustained on orbits typical of EVs between times 20 and 100 Myr by the MB group (Fig. 12b). Figure 12b also shows that the HU population has a rapid and short production of EV bodies since, as already noted, HU members first become EV as a result of a decrease of their orbital inclination and then become EC. Conversely, the number of EVs sustained by the MB group increases slowly because they first become EC and then decrease their semimajor axis below 2 AU due to planetary encounters. A decrease of their eccentric-

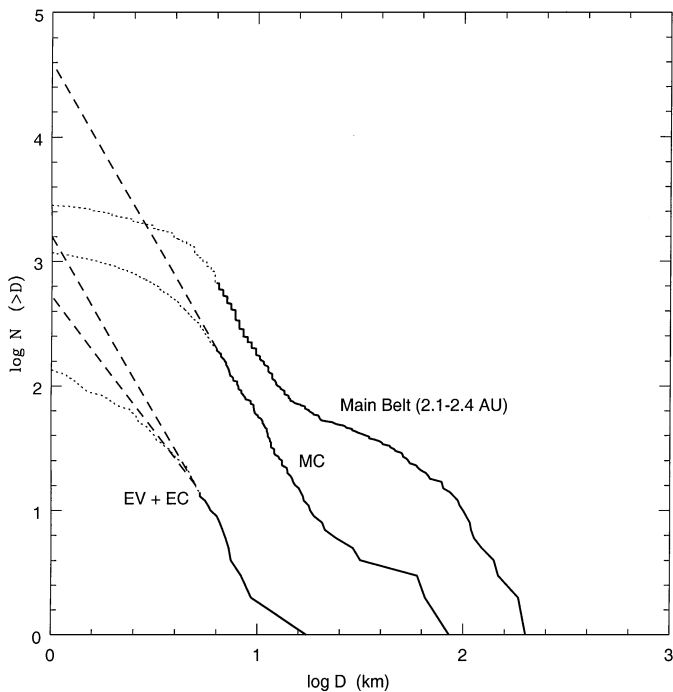
ity due to close encounters and/or resonances raises again their perihelion distance above 1 AU so that they become EV.

Figure 12 is actually computed directly from the evolutions of the MC groups on 100 Myr. Consequently, it does not simulate a steady-state scenario. In such a scenario, half of each group should be regenerated for every time corresponding to their median lifetime (e.g., every 60 Myr for the MB group). In that case, a low estimate of the average steady-state populations of ECs and EVs can be obtained by adding to their average number in the 60- to 100-Myr range (3 ECs and 1 EV) half the average numbers supplied by the MB population during the first 60 Myr (2 ECs and 1 EV). The conclusion that Mars-crossers are the dominant source of multikilometer Earth-crossers (Migliorini *et al.* 1998) must then be reconsidered, since our computation suggests that they are actually able to maintain about half of the current 10 ECs with diameter larger than 5 km. Of course, one may argue that the threshold value of the diameter at which observations of the Mars-crosser population are complete may be larger than 5 km and, therefore, increasing the number of MCs down to this size would increase the number of ECs accordingly. However, unless observations are still biased against a large component of MCs with diameter larger than 5 km, complementary sources and/or mechanisms may be required to sustain the remaining number of big ECs. This is still an open problem since, based on our current understanding of collisional processes, we estimate that catastrophic disruptions of main belt bodies close to strong resonances such as the 3/1 and  $\nu_6$  resonances, cannot generate half of the population of ECs with diameter larger than 5 km on the time scale required to maintain them in a steady state (we recall that the median lifetime of bodies injected into such resonances is only about 2 Myr; see Gladman *et al.* (1997)). Also, though the contribution of comets cannot be disregarded, other mechanisms, such as drifts in semimajor axis caused by the Yarkovsky effect or by close encounters with the largest asteroids (e.g., 1 Ceres), could also contribute to the injection of large bodies in the strong resonances. We leave a more detailed discussion of this issue for the Conclusion (Section 7).

## 5. RELATING ORBITAL PROVENANCE TO STATISTICS OF PHYSICAL TYPES

It has been generally accepted (Mc Fadden *et al.* 1988, Lupishko and Di Martino 1998) that the EC population represents a mixture of taxonomic types which fits quite well the relative abundances found in the whole main belt (taking into account the most important observational biases).

In the previous sections, we have shown that Mars-crossers are an important intermediate source of the ECs larger than 5 km. Furthermore, in Fig. 13 we plot the cumulative size distribution of the known population of Mars-crossers and compare it to that of inner main belt asteroids ( $2.1 < a < 2.4$  AU) and to that of the population including EC and EV asteroids. Since our dynamical results show that there is an interchange of objects between ECs and EVs, these groups can be also considered as a unique



**FIG. 13.** Cumulative size distributions (log-log scale) of main belt asteroids with  $2.1 < a < 2.4$  AU, Mars-crossers (MC), and the population including ECs and EVs (EC+EV). The distributions are drawn in full lines up to the completeness limit in diameter. Extrapolations at smaller sizes are represented by straight dashed lines. The same slope is used ( $-2.9$ ) for the extrapolation line of the MC distribution and for the upper line of the EC+EV distribution. The lower extrapolation line of the EC+EV distribution ( $-2.1$ ) is derived from Rabinowitz (1996). See text for details.

population. One can see in Fig. 13 that the cumulative size distributions of both main-belt and Mars-crossing asteroids can be extrapolated at small sizes with straight lines having the same slope ( $\approx -2.9$ ). Note, however, that some recent works suggest that the slope of these distributions becomes shallower at small sizes (see, e.g., Jedicke and Metcalfe 1998). Nevertheless, the apparent similarity of the size distributions supports the idea, already explored by Migliorini *et al.* (1998) and Morbidelli and Nesvorný (1999), that Mars-crossers are a subpopulation of previously main-belt asteroids (see also Section 6). For EV and ECs, we have considered two slopes which can be considered as upper and lower limits of (EC+EV) cumulative size distributions at small sizes: one slope is similar to the size distribution of the Mars-crossers, and the other slope ( $\approx -2.1$ ) is derived from Rabinowitz (1996) for the Earth-crossers, defined in this case as the real ECs plus half of the Amor asteroids.

According to these extrapolations, the estimated number of Mars-crossers with diameters  $D > 2$  km is 5,000. Since our simulations suggest that the Mars-crossers can sustain a population of (EC+EV)s that is about 2.5% (about 1.5% for ECs and about 1% for EVs) of the total number of the MC population, the Mars-crossers can sustain 125 (EC+EV)s with  $D > 2$  km. Similarly, for  $D > 1$  km, there are 40,000 Mars-crossers which can

sustain 1000 (EC+EV)s. According to the extrapolation of the size distributions of (EC+EV)s with the two lines defined above, the number of (EC+EV)s with  $D > 2$  km could be in the range 120 to 250, whereas that with  $D > 1$  km could be in the range 500 to 2000. These estimates, which are derived from a “crude” extrapolation of the observed populations, support the possibility that Mars-crossers could also be an important intermediate source of ECs larger than 1 km. Note that, since our simulations suggest that they should only sustain half of the ECs with  $D > 5$  km, the result that they can sustain the total number of ECs with  $D > 1$  km may be an artifact due to the extrapolation with these different slopes of the size distributions of (EC+EV)s and MCs. Decreasing our estimated number of Mars-crossers with  $D > 1$  km would indeed decrease their production of ECs with  $D > 1$  km.

Since most ECs with known taxonomic types have a diameter  $D > 2$  km (70% of ECs with semimajor axis  $< 2$  AU and 100% of ECs with  $a > 2$  AU), if a substantial fraction comes from the Mars-crossing population, then their taxonomic distribution should reflect that of the various groups of Mars-crossers. To check this, we have to take into account the relative number of Mars-crossers of different groups, the taxonomic distribution inside each group, and the efficiency by which each group sustains the Earth-crossing population.

The PH and MB2 Mars-crossers rarely evolve to the region with  $a < 2$  AU, and it is convenient to divide the Earth-crossers in two classes according to this threshold. Moreover, the first class ( $a < 2$  AU) is the one able to exchange objects with the EV population, and its lifetime is considerably longer than that of the second class ( $a > 2$  AU). We also divide the MB population into two subgroups (those with either  $a < 2.5$  AU or  $a > 2.5$  AU) in order to take into account the diversity of taxonomic types observed below and above this limit, as well as the difference of efficiency in sustaining the EC and EV populations. In summary, we consider five source populations (MBs with  $a < 2.5$  AU, MBs with  $a > 2.5$  AU, HUs, PHs, and MB2s, hereafter denoted  $k = 1, \dots, 5$ ) and three target populations (ECs with  $a > 2$  AU, ECs with  $a < 2$  AU, and EVs, hereafter denoted  $j = 1, \dots, 3$ ).

To estimate the relative populations in the different source regions, we have restricted our considerations to the number of bodies larger than 5 km, in order to reduce as much as possible the consequences of observational biases. The albedos that we have assumed to estimate the diameters are those reported in Table I. Nevertheless, even 5 km is beyond the completeness limit at  $a > 2$  AU. In order to approximately compensate for this bias, we have multiplied the number of 5-km bodies reported in Table I by 1.5 in the region  $2 < a < 2.5$  AU and by 3 in the zone  $2.5 < a < 2.8$  AU. These multiplying factors come from a comparison of the observed asteroids of 5 km and those expected on the basis of a linear extrapolation of the observed size distribution down to 5 km.

For each source, we have deduced from the simulations the average fraction  $F_{\text{esc}}(k)$  of the integrated population that escapes from the source region per million year. Since this number slowly

**TABLE II**  
**Data Used for the Spectral Analysis**

Source	$N_{\text{esc}}$	$T_{\text{res}}(1)$	$T_{\text{res}}(2)$	$T_{\text{res}}(3)$	$S/O$	$S/C$
MB ( $a < 2.5$ AU)	2.66	0.66	2.24	1.15	17/3	17/3
MB ( $a > 2.5$ AU)	8.40	0.47	0.34	0.01	4/7	4/3
HU	0.04	1.94	8.02	21.70	5/7	5/2
PH	0.26	3.06	2.11	0.11	13/1	13/1
MB2	0.22	0.98	0.	0.	2/4	2/2

*Note.* We have restricted our considerations to the number of bodies larger than 5 km (corrected by the multiplying factors defined in the text). For each source region,  $N_{\text{esc}}$  ( $\text{Myr}^{-1}$ ) is the number of particles escaping from the source,  $T_{\text{res}}(j)$  ( $\text{Myr}/\text{particle}$ ) is the residence time in each target region ( $j = 1, \dots, 3$ , are, respectively, EC with  $a > 2$  AU, EC with  $a < 2$  AU, and EV), and the ratios  $S/O$  and  $S/C$  are the ratios of known taxonomic types in the source region (S-types/Other types, and S-types/C-types).

decays with time because the source population is not kept in steady state in the simulation, we measure  $F_{\text{esc}}(k)$  in the first part of the integration, when it stays approximately constant. By multiplying  $F_{\text{esc}}(k)$  by the total estimated number of objects larger than 5 km, we finally estimate the number  $N_{\text{esc}}(k)$  of asteroids larger than 5 km that escape from each source region, per Myr. The numbers are reported in column 2 of Table II. We assume that their ratio would be unchanged if different size ranges were considered. Note that in Table II, the reported number of escaping bodies per Myr from the MB group with  $a > 2.5$  AU is much greater than the one from the MB group with  $a < 2.5$  AU due to the adopted multiplying factor equal to 3 for the first group and to 1.5 for the second one. Decreasing the completeness limit to 5 km would then result in a smaller contribution of the first group. As we shall see, this may explain some of the differences between the computed and the observed ratios of taxonomic types in the target regions.

As for the distribution of taxonomic types inside each source region, we define the ratio  $S/O(k)$  between the number of bodies that are S-type and the number of bodies that are of taxonomic type other than S. Similarly we define a ratio  $S/C(k)$  between the number of S-type asteroids and the number of bodies of dark taxonomic type (C, D, F or G). The ratios  $S/O(k)$  and  $S/C(k)$  for each source population are shown in the two last columns of Table II.

Finally, from our simulations, we have computed for each source population the mean time  $T_{\text{res}}(k, j)$  spent inside the target region  $j$  by the asteroids who escaped from the source region  $k$ . These times are shown in columns 3, 4, and 5 of Table II.

With all these data in hand, the expected ratios  $S/O(j)$  and  $S/C(j)$  inside each target population are given by the formula

$$X/Y(j) = \frac{\sum_{k=1}^5 N_{\text{esc}}(k) T_{\text{res}}(k, j) (X/N_{\text{Tax}})(k)}{\sum_{k=1}^5 N_{\text{esc}}(k) T_{\text{res}}(k, j) (Y/N_{\text{Tax}})(k)},$$

where  $X$  and  $Y$  are the considered taxonomic types and

$N_{\text{Tax}}(k) = S(k) + O(k)$  is the total number of asteroids with known spectral type in the source region  $k$ . We now apply this formula and compare the results obtained by its evaluation with the observational data of each target group. Using data from both Tholen (1988) and Xu *et al.* (1995), we have taxonomic types of 31 asteroids in the MB group, 14 in the PH one, 6 in the MB2 one, 12 in the HU one, and 65 in the EC+EV groups.

*EC population with  $a > 2$  AU.* The expected ratios are  $S/O(1) = 1.25$  and  $S/C(1) = 1.81$ . The observed population of EC with  $a > 2$  AU has ratios  $S/O$  and  $S/C$  of 1.7 and 2.3, respectively. Compared to the expected ratio, the observed population shows a slightly greater excess of S-type with respect to other taxonomic types. Recall, however, that we have used a multiplying factor of 3 to compute the number of escaping bodies from the MB group with  $a > 2.5$  AU which contains a great fraction of dark bodies. If this correction is too large, we may then have overestimated their contribution, increasing thus the expected abundance of dark-type bodies in the target region.

*EC population with  $a < 2$  AU.* The expected ratios are  $S/O(2) = 2.296$  and  $S/C(2) = 3.3$ , whereas the observed ones are 2.9 and 5.2, respectively. As mentioned previously, though there are no drastic differences, we expect a slightly greater fraction of dark-type objects than the fraction given by the observed population.

*EV population.* The expected ratios are  $S/O(3) = 2.95$  and  $S/C(3) = 4.4$ , in comparison with the observed values of 1.8 and 5.5, respectively. In this case, there is a small excess of other types of objects in the observed population. Interestingly, the observed population still shows a small lack of C-type objects but has an excess of other types of objects. They correspond mainly to E-type asteroids which share the same taxonomic type as Hungaria asteroids. This is consistent with the already discussed potential link between EVs and HU asteroids, but this also shows that the HU may contribute even more than is expected from our simulations.

*Joined EV and EC ( $a < 2$  AU) populations.* Since our dynamical results have shown that there is an interchange of objects between the EV and EC ( $a < 2$  AU) populations, we consider here these two populations as a unique one. The general formula can be easily adapted by adding  $T_{\text{res}}(k, 2)$  and  $T_{\text{res}}(k, 3)$ . The expected ratios then result in  $S/O = 2.47$  and  $S/C = 3.58$ , again in fairly good agreement with the observed ones of 2.5 and 5.3, respectively, and still with a small lack of dark-type objects in the observed population.

Note that these results must be interpreted with caution. Indeed, they rely on many assumptions and biases. Moreover, they are obtained with a relatively limited number of objects with well-defined taxonomic types. Note, however, that new data supplied by Bus (private communication) give similar ratios.

It is very encouraging that the rough computation above gives an expected population of EC and EV asteroids which is at

least not in drastic disagreement with the observed one. If supported by future data, this would confirm, on the basis of physical properties, that Mars-crosser asteroids are an important source of large EC+EV (as already found from a dynamical point of view).

## 6. WHERE DO MARS-CROSSERS COME FROM?

Until now, we have studied the interrelation between the Mars-crossing populations, the Earth-crossers, and the EV Mars-crossers. But obviously, the Mars-crossers must be a sort of intermediate source, which itself needs to be kept in steady state by much larger source populations of non-planetary-crossing asteroids.

In Migliorini *et al.* (1998), we have provided a tentative explanation. The fact that the MB, HU, and PH groups have semimajor axes and inclinations very similar to those of three crowded populations of asteroids that do not cross the orbit of Mars (main belt, Hungarias, and Phocaeas) suggests that these populations might be continuously losing objects to the Mars-crossing region. As a confirmation, we have shown with a 100-Myr numerical integration that most asteroids in the high eccentricity part of the inner asteroid belt ( $2.1 < a < 2.5$  AU) are unstable. A big majority of the integrated bodies slowly increase their proper eccentricity, showing a phenomenon of chaotic diffusion, and an important fraction of them become Mars-crossers within 100 Myr. The number of bodies escaping from the inner belt seems to be large enough to keep the MB Mars-crossing population in steady state, at least for the next 60 Myr. Morbidelli and Nesvorný (1999) have investigated in detail this diffusion process, and they found that it is mainly due to the presence of a large number of outer mean motion resonances with Mars (4/7, 7/13, . . .), high-order mean motion resonances with Jupiter (7/2, 10/3, . . .), and three-body resonances with Jupiter and Saturn.

It is therefore important to compare the taxonomic distributions of Mars-crossing and non-Mars-crossing asteroids located in the same region of semimajor axis and inclination, in order to check whether the Mars-crosser population is similar to the non-Mars-crossing one.

For the non-Mars-crossing *Hungaria* asteroids, the ratio  $S/O$  is about 0.5, close to the 0.7 value found for the HU Mars-crossers. Note that in this region, the majority (more than 90%) of the non-S-type objects are characterized as E- or X-types. We recall that X-type bodies could be in reality E-types with non-measured albedo. Consequently, as several authors (see, e.g., Zellner *et al.* 1985) have already noted, there exists an overabundance of E-type asteroids in the *Hungaria* region. Inside this region, three probable families coexist (Forzoni Accolti 1995). The largest one is connected with the asteroid (434) *Hungaria*, and all of its seven characterized members belong to the E- or X-type. The two other small families have classified objects belonging to the S type (three bodies). One can argue that the disruption of an E-type parent body may have created the subse-

quent local overabundance of this otherwise not very common taxonomic type. However, the E-type family is quite far from the Mars-crossing region, so it is unlikely that the E-type HU Mars-crossers have been injected into the Mars-crossing region as a result of the catastrophic breakup of the family. This scenario would therefore imply that a diffusion process has transferred some family objects to the Mars-crossing region. On the other hand, one can also argue that the original population of HU was already composed by a mixture of S- and E-type asteroids (with an overabundance of this last type) and that one of the largest E-type objects was collisionally disrupted and formed the family. In this scenario, since the overabundance of E-type would be original and not only due to the disruption which formed the family, the E-type Mars-crossers would not need to have any connection with the family members. Further studies are required to privilege one of the two options.

The MB group with  $a < 2.5$  AU has a ratio  $S/O$  equal to 5.7, which is in good agreement with that of the non-Mars-crossers with  $2 < a < 2.3$  AU. This last is equal to 6.0 if only one object per family is considered. This last restriction is necessary in order not to be biased by the fact that family members have been observed much more than background objects. On the other hand, the non-Mars-crossers with  $2.3 < a < 2.5$  AU (again considering only one object per family) have a much smaller ratio of 0.7, showing an overabundance of asteroids of non-S-type (mainly dark types, like C and F). This overabundance does not appear in the corresponding, but very small, Mars-crossing sample of taxonomic types. Moreover, we have to recall that in the region  $2.3 < a < 2.5$  AU, three large families exist and are located at a large enough eccentricity to suggest that their members are serious candidates for diffusing into the Mars-crossing zone (Erigone, Polana, and Nysa families). The Erigone and Polana families are surely dark-type families (C and F, respectively). Therefore, one can argue that their presence can partially affect the background objects, but it can not affect the region of Mars-crossers yet or any longer. Another explanation could be that many of the S-type Mars-crossers with  $2.3 < a < 2.5$  AU actually diffused from the main belt with  $2 < a < 2.3$  AU, in which this type is more abundant and the diffusion is more efficient, and then were moved to higher semimajor axis due to shallow Mars encounters. On the other hand, the Nysa family, located in the region  $2.3 < a < 2.5$  AU and the closest to the Mars-crossing zone, seems also to be composed of S-type objects. There is also evidence that it could be relatively young. A study on these two points regarding of the Nysa family is in progress (Doressoundiram *et al.*, in preparation). The abundance of S-type objects found in the Mars-crosser population may then mainly reflect the diffusion of bodies belonging to the Nysa family. Again further studies on the dynamical evolution of these families will help us to better understand the diffusion process as well as to estimate their age.

Concerning the MB group with  $a > 2.5$  AU, the ratio  $S/O$  is 0.6 in excellent agreement with that of the non-Mars-crosser sample (0.7).

The PH region is mainly composed of S-type objects both inside and outside the Mars-crossing zone.<sup>1</sup>

Finally, the MB2 group shows a ratio  $S/O$  of 0.5, which also fits quite well that of the MB one with  $a > 2.5$  (i.e., in the same region of semimajor axis but at lower inclinations), but it does not fit that of the non-Mars-crossers in the same inclination region. These last have indeed a much lower ratio  $S/O$  of 0.15. Whether this value represents a real misfit is difficult to decide, due to the very small number of spectroscopically characterized MB2 Mars-crossers.

## 7. CONCLUSION

We have classified the Mars-crossing asteroids in different groups depending on their current inclination and semimajor axis, and we have shown that each group has its own typical dynamical evolution, lifetime, and end-states. The MB, HU, and PH groups appear to be an important reservoir of multikilometer Earth-crossers. By using the numerical integrations of the complete sample of observed Mars-crossers, we have computed the expected orbital distribution of NEAs coming from each of the Mars-crossing groups, as well as the number of Earth-crossers larger than 5 km in size, that they can sustain in a steady-state scenario. We have thus shown that they are able to sustain at least half of the observed Earth-crossing population with diameter larger than 5 km. The EV group is composed of objects which previously belonged to either the MB or the HU group. For all Mars-crossing groups, the dominant mechanism for becoming an Earth-crosser is injection into a resonance as a result of close approaches with Mars. The asteroids that become Earth-crossers with  $a > 2$  AU have typically a subsequently short lifetime, being either ejected by Jupiter's encounters toward the outer Solar System or forced by a strong resonance to collide with the Sun. The asteroids that become Earth-crossers with  $a < 2$  AU, or manage to migrate into this region by the effects of Earth encounters, survive longer. In the region  $a < 2$  AU, there is a continuous interchange between the Earth-crossing and the EV Mars-crossing populations. A nonnegligible fraction of these populations eventually temporarily penetrate into the Aten region ( $a < 1$  AU) and even reach the region completely inside Earth's orbit.

Since our results suggest that the Mars-crossers are able to sustain only half the population of Earth-crossers with diameter larger than 5 km, there is still a missing link between Earth-

crossers and their potential sources. Actually, the real scenario for the origin of Earth-crossers should consist of the contribution of several sources such as main belt bodies injected in different resonances and Mars-crossers coming themselves from the main belt through high-order resonances. The proper combination of these sources may also depend on the considered interval of diameters of the asteroids. Previous studies (Menichella *et al.* 1996) suggest that the source of subkilometer Earth-crossers could be main belt asteroids injected into strong resonances which increase their orbital eccentricity, such that they are led to Earth-crossing orbits. For subkilometer bodies, the number and frequency of collisions between asteroids close to these resonances seems sufficient to generate the required amount of material at the appropriate rate. Conversely, for bodies with diameter larger than 1 to 2 km, the collisional scenario may not be valid anymore since the number of potential parent bodies close to resonances and the frequency of their breakup allowing the generation of multikilometer fragments cannot occur with the required high frequency (recall that 2 Myr is the median lifetime of injected bodies in main belt resonances leading to Earth-crossing orbits). This was the reason that Migliorini *et al.* (1998) looked at the Mars-crossers as the dominant source of Earth-crossers. However, if the Mars-crossers are able to sustain half of the population of Earth-crossers with diameter greater than 5 km, some other mechanisms still need to be found. Recent studies have shown that nongravitational mechanisms such as the Yarkovsky effect can cause a secular drift in semimajor axis of small bodies, allowing them to get closer to a resonance and then be injected and driven to Earth-crossing orbits (Farinella and Vokrouhlický 1999). The time scale of the drift and the efficiency of this thermal mechanism depends on several physical parameters (e.g., thermal properties of the body, orientation of its spin-axis) and on the size of the asteroid. In particular, it is debatable whether its efficiency would be enough to explain the origin of the remaining part of the population of Earth-crossers with diameter larger than 5 km. Some other undiscovered mechanisms may still exist; the contribution of extinct comets may also be considered in Earth-crossing orbits, and it may also be that our understanding of already known mechanisms is still too poor.

Things get even worse if we consider recent studies (Rabinowitz *et al.* 2000, Bottke *et al.* 1999) suggesting that the slope of the debiased size distribution of Earth-crossers with diameter larger than 100 m may even be shallower than the much steeper slopes of the size distributions of fragments resulting from collisions (Tanga *et al.* 1999). If this result is confirmed, it will mean that even in the 100 m–1 km range, the collisions are not the dominant mechanism injecting small main belt bodies into resonances; otherwise their size distribution in the Earth-crossing region should follow the same slope as the original one. Therefore, other mechanisms of injection into resonances involving shallower size distributions would be necessary to overwhelm the production through collisions (which in any case occur!). Again, the Yarkovsky effect could be an efficient mechanism injecting subkilometer bodies into resonances, and

<sup>1</sup> However, there is an important point that we need to address. In this region, two major families have actually been found (Forzoni Accolti 1995). They are associated with (24) Phocaea and (1310) Villigera. Both families include a large percentage of Mars-crosser objects. Indeed, they contain 20 (over 123 members) and 24 (over 27) Mars-crossers, respectively. Among these, only one became EC after 100 Myr, while the others have been found "stable" over the 100-Myr integration time span. One can argue that, even inside the Mars-crossing region, both families were not seriously depleted on time scales of 100 Myr, and that a member escapes and becomes EC only sporadically, but the overall structure is not very much affected. It follows that the age of these families cannot be seriously constrained on the basis of this slow chaotic mechanism.

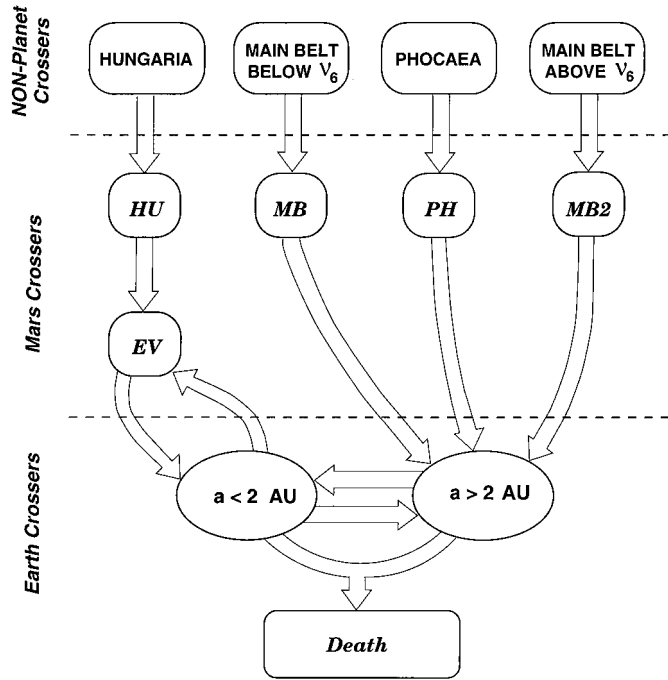


**FIG. 14.** Schematic view of the new scenario of the origin of Mars-crossers and their subsequent evolution to Earth-crossing orbits. The HU, PH, MB, and MB2 Mars-crossers are sustained, respectively, by the non-planet-crossing asteroids of the Hungaria, Phocaea, and main-belt (below and above the  $\nu_6$  resonance) populations. In turn, they supply some fraction of the Earth-crossers and EV Mars-crossers. The arrows denote the main fluxes among the populations.

some other mechanisms may also be required. This will need further investigations.

Nevertheless, considering that MB, HU, PH, and MB2 Mars-crossers are, anyway, an important intermediate reservoir of both multikilometer Earth-crossers and EV Mars-crossers, we have computed the expected spectral taxonomic distribution of the latter and compared it with the observational data. Although many problems are still open and require specific studies, the overall comparison is quite satisfactory, showing that at least no relevant contradictions are raised by the spectral data.

Similarly, we have checked that the abundances of different spectral types in the MB, HU, and PH Mars-crossing groups are in good agreement with the spectral abundances of asteroids in the main-belt, Hungaria, and Phocaea regions, thus supporting the scenario that the latter are the source reservoirs of MBs and HUs (Migliorini *et al.* 1998, Morbidelli and Nesvorný 1999). Discrepancies exist only in the comparison between the spectral distributions in the MB2 group and in the main belt beyond 2.5 AU and above the  $\nu_6$  resonance, but the data statistics are very poor in this case.

In conclusion, in light of our dynamical and spectroscopical considerations, the overall scenario, which still needs some quantitative refinement, for the origin of Mars-crossers and their subsequent evolution to Earth-crossing orbits is the one sketched in Fig. 14.

## ACKNOWLEDGMENTS

We thank A. Cellino, P. Tanga, and S. J. Bus for useful discussions, and R. Greenberg and D. Nesvorný for their constructive reviews. We are also very grateful to W. Bottke for providing data. P. Michel has worked on this project partly while staying at the Turin Astronomical Observatory thanks to an external fellowship of the European Space Agency.

## REFERENCES

- Bottke, W. F., R. Jedicke, A. Morbidelli, B. Gladman, and J. M. Petit 1999. Understanding the distribution of near-Earth asteroids. *Bull. Am. Astron. Soc.* **31**, 1116–1116.
- Bottke, W. F., M. C. Nolan, H. J. Melosh, A. M. Vickery, and R. Greenberg 1996. Origin of the spacewatch small Earth-approaching asteroids. *Icarus* **122**, 406–427.
- Bowell, E., K. Muinonen, and L. H. Wasserman 1994. A public-domain asteroid orbit data base. In *Asteroids, Comets, Meteors* (A. Milani, M. Di Martino, and A. Cellino, Eds.), pp. 477–481. Kluwer, Dordrecht.
- Farinella, P., and D. Vokrouhlický 1999. Semimajor axis mobility of asteroidal fragments. *Science* **283**, 1507–1510.
- Forzoni Accolti, E. 1995. *Identificazione statistica delle famiglie di asteroidi ad alta inclinazione e/o ad alta eccentricità*. Ph.D. dissertation, Università degli studi di Torino, Facoltà di Scienze M.F.N., Turin, Italy.
- Gladman, B., P. Michel, and Ch. Froeschlé 2000. The near-Earth object population. *Icarus*, in press.
- Gladman, B., F. Migliorini, A. Morbidelli, V. Zappalà, P. Michel, A. Cellino, Ch. Froeschlé, H. Levison, M. Bailey, and M. Duncan 1997. Dynamical lifetimes of objects injected into asteroid belt resonances. *Science* **277**, 197–201.
- Greenberg, R., and C. R. Chapman 1983. Asteroids and meteorites—Parent bodies and delivered samples. *Icarus* **55**, 455–481.
- Greenberg, R., and M. Nolan 1989. Delivery of asteroids and meteorites to the inner Solar System. In *Asteroids II* (R. P. Binzel, T. Gehrels, and M. S. Matthews, Eds.), pp. 778–804. Univ. of Arizona Press, Tucson.
- Jedicke, R., and T. F. Metcalfe 1998. The orbital and absolute distributions of main belt asteroids. *Icarus* **131**, 245–260.
- Levison, H. F., and M. J. Duncan 1994. The long-term dynamical behavior of short-period comets. *Icarus* **108**, 18–36.
- Lupishko, D. F., and M. Di Martino 1998. Physical properties of near-Earth asteroids. *Planet. Space Sci.* **46**, 47–74.
- McFadden, L. A., D. J. Tholen, and J. G. Veeder 1988. Physical properties of Aten, Apollo and Amor asteroids. In *Asteroids II* (R. P. Binzel, T. Gehrels, and M. S. Matthews, Eds.), pp. 442–467. Univ. of Arizona Press, Tucson.
- Menichella, M., P. Paolicchi, and P. Farinella 1996. The main belt as source of near-Earth asteroids. *Earth Moon Planets* **72**, 133–149.
- Michel, P. 1997. Effects of linear secular resonances in the region of semimajor axes smaller than 2 AU. *Icarus* **129**, 348–366.
- Michel, P., and Ch. Froeschlé 1997. The location of linear secular resonances for semimajor axes smaller than 2 AU. *Icarus* **128**, 230–240.
- Michel, P., P. Farinella, and Ch. Froeschlé 1998. Dynamics of Eros. *Astron. J.* **116**, 2023–2031.
- Michel, P., R. Gonczy, P. Farinella, and Ch. Froeschlé 1999. Dynamical evolution of 1036 Ganymed, the largest near-Earth asteroid. *Astron. Astrophys.* **347**, 711–719.
- Michel, P., V. Zappalà, A. Cellino, and P. Tanga 2000. Estimated abundances of Atens and asteroids evolving on orbits between Earth and Sun. *Icarus* **143**, 421–424.
- Migliorini, F., P. Michel, A. Morbidelli, D. Nesvorný, and V. Zappalà 1998. Origin of multikilometer Earth and Mars-crossing asteroids: A quantitative simulation. *Science* **281**, 2022–2024.

- Morbidelli, A., and B. Gladman 1998. Orbital and temporal distributions of meteorites originating in the the asteroid belt. *Meteoritics Planet. Sci.* **33**, 999–1016.
- Morbidelli, A., and D. Nesvorný 1999. Numerous weak resonances drive asteroids toward terrestrial planets' orbits. *Icarus* **139**, 295–308.
- Rabinowitz, D. L. 1996. Observations constraining the origins of Earth approaching asteroids. In *Completing the Inventory of the Solar System* (T. W. Rettig and J. M. Hahn, Eds.), A.S.P. Conf. Ser. 107, pp. 13–28. A.S.P., San Francisco.
- Rabinowitz, D. L., E. Helin, K. Lawrence, and S. Pravdo 2000. A reduced estimate of the number of kilometre-sized near-Earth asteroids. *Nature* **403**, 165–166.
- Tanga, P., A. Cellino, P. Michel, V. Zappalà, P. Paolicchi, and A. Dell'Oro 1999. On the size distribution of asteroid families: The role of geometry. *Icarus* **141**, 65–78.
- Tholen, D. J. 1988. Asteroid taxonomic classification. In *Asteroids II* (R. P. Binzel, T. Gehrels, and M. S. Matthews, Eds.), pp. 1139–1150. Univ. of Arizona Press, Tucson.
- Wetherill, G. W. 1985. Asteroidal source of ordinary chondrites. *Meteoritics* **20**, 1–22.
- Wetherill, G. W. 1987. Dynamic relationships between asteroids, meteorites, and Apollo-Amor objects. *Philos. Trans. R. Soc. London* **A323**, 323–337.
- Wetherill, G. W. 1988. Where do the Apollo objects come from? *Icarus* **76**, 1–18.
- Xu, S., R. P. Binzel, T. H. Burbine, and S. J. Bus 1995. Small main-belt asteroid spectroscopic survey: Initial results. *Icarus* **115**, 1–35.
- Zellner, B., D. J. Tholen, and Tedesco, E. F. 1985. The eight-color asteroid survey: Results for 589 minor planets. *Icarus* **61**, 355–461.